Optical and Electrical Detection of Single Molecule Translocation through Carbon Nanotubes

Weisi Song[1,2], **Pei Pang**[1], **Jin He**[4], and **Stuart Lindsay**[1,2,3,*]

[1]Biodesign Institute, Arizona State University, Tempe, AZ 85287

[2]Department of Physics, Arizona State University, Tempe, AZ 85287

[3]Department of Chemistry and Biochemistry, Arizona State University, Tempe, AZ 85287

[4]Department of Physics, Florida International University, Miami, FL 33199

Abstract

Ion current through a single-walled carbon nanotube (SWCNT) was monitored at the same time as fluorescence was recorded from charged dye molecules translocating through the SWCNT. Fluorescence bursts generally follow ion-current peaks with a delay time consistent with diffusion from the end of the SWCNT to the fluorescence collection point. The fluorescence amplitude distribution of the bursts is consistent with single molecule signals. Thus each peak in the ion current flowing through the SWCNT is associated with the translocation of a single molecule. Ion current peaks (as opposed to blockades) were produced by both positively (Rhodamine 6G) and negatively (Alexa 546) charged molecules, showing that the charge filtering responsible for the current bursts is caused by the molecules themselves.

Keywords

Nanopores; dye translocation; single molecule fluorescence; carbon nanotubes; nanopore ion current

Carbon nanotubes have some unique properties as nanofluidic devices.[1–14] The flow of water inside them is almost frictionless[8] and they can be small enough to give a high degree of molecular selectivity, based on size exclusion.[1, 5] A small amount of charge in the vicinity of the nanotube wall results in a large electroosmotic flux of electrolyte because of the small friction. This large flux can give rise to very large ionic currents if there is any imbalance between the concentration of anions and cations in the tube.[8] Such an imbalance may be caused by charged groups at the entrance to the tube. For example, carboxylate residues are negatively charged at neutral pH, so favor entry of cations over anions.[8] One unexpected consequence of this effect is that the translocation of molecules through the tube can be marked by large increases in ion current through it.[6, 7] In contrast, in larger channels, where electrophoresis dominates ion current, the translocation of a molecule is signaled by a decrease in current because the molecule blockades ion flow.[15] A simulation of DNA translocation through a carbon nanotube shows that the increase in ion current is a consequence of an additional, even larger charge imbalance inside the nanotube caused by repulsion of anions by the intrinsic charge on the DNA.[16] Our interest in DNA translocation

was motivated by the possibility of nanopore sequencing,[17] using the CNT both as an electrically-conducting nanopore and as a device that might enable control of translocation speed. We were able to use the quantitative polymerase chain reaction[7] (q-PCR) to establish a correlation between the number of ion current peaks and the amount of DNA translocated, but the errors in qPCR data can be quite large. Thus we have sought a better method of correlating molecular translocations with features in the ion current signal. To this end, we have built single nanofluidic channels with single-walled carbon nanotubes (SWCNT) using an optical microscope cover glass as the base for the device, as illustrated in Figure 1A. To build the nanofluidic channel, we transfer SWCNTs from a conventional silicon wafer onto a microscope cover glass patterned with index markers (Figure S1). An SEM image locates the SWCNTs relative to these markers (Figure 1B) for subsequent lithographic formation of a barrier separating two fluidic channels that contact the ends of the SWCNT. The SWCNTs are opened in the reservoirs by exposure to an oxygen plasma, leaving the SWCNT under the barrier intact. The device is operated under laser illumination with fluorescence signals collected by a high numerical aperture objective lens, similar to a recent study of diffusion in mesoporous silica.[18] This instrument is capable of detecting single dye molecules by means of the fluorescence they emit as they pass through the laser beam. Dye molecules are placed into an input chamber on one side of the SWCNT channel and the laser is focused into a chamber on the other side of the SWCNT nanochannel. If no current flows through the junction, no fluorescence is observed on the output side. However, if a current flows (with dye molecules in the input chamber) then bursts of fluorescence are observed in the output chamber. These bursts follow the ion current pulses with a short delay consistent with the time taken to diffuse from the end of the SWCNT to the laser illumination point. Thus this result shows that each peak in the ion current marks the passage of one dye molecule, both for positively (Rhodamine 6G) and negatively (Alexa 546) charged molecules.

Results and Discussion

We first verified that ionic current flow through the devices was through the SWCNTs and not by means of a leakage path. We did this with control devices lacking SWCNTs under the barrier, or with SWCNTs but unopened by an oxygen plasma. None of these control devices showed any measureable conductance. The strongest evidence for conductance *via* electroosmotic flow in a SWCNT comes from the unusual dependence of conductance on salt concentration observed in SWCNT devices.[7, 8] We have consistently observed this form of power law for ion transport through small-diameter SWCNTs. As we have explained in previous reports[7,8], it is likely a consequence of significant electroosmotic flow in a very small frictionless channel and can be explained in terms of the dependence of the net excess charge in the tube on the bulk salt concentration. In contrast to conventional nanopores, which show little concentration dependence at low salt, owing to fixed surface charge[19] the conductance of SWCNTs changes most rapidly at low salt, as illustrated by data (Figure 2) taken with one of the cover-glass devices used for dye translocation.

As was the case for DNA[7], only a minority (~10%) of the devices gave signal spikes after dye was added to the input reservoir. This variability probably reflects variations in SWCNT chirality as well as device to device variation in surface charge near the tube openings. However, in devices that did generate signals after dye addition, almost all of the spikes (>90%) corresponded to an increase in ion current passing through the tube (Figure 3A, Alexa 546, Figure 4A Rhodamine 6G – note negative current increases downwards). The spike amplitudes and widths depended upon the particular tube being used, but it was typically a few tens of pA with a width >0.1s (Table 1 and Figures S2–3). No fluorescence signals were seen in devices lacking dyes or without the driving bias (0.4 to 0.5V) applied. The appearance of ion current spikes was accompanied by distinct bursts of fluorescence (Figures 3B and 4B). Note that the noise background in the case of Alexa 546 fluorescence

measurements was a little larger because we used a larger pinhole (150μm) than that used in the later R6G measurement (50μm). The stochastic distribution of fluorescence signals introduces an element of guesswork into associating a particular ion current spike with a fluorescence burst (red arrows) but the fluorescence appears to follow the ion current spike with a delay of a fraction of a second (Figures 3C, 4C). Measured distributions of these delay times for two experiments are shown in Figures 3D and 4D.

The electric field outside of the carbon nanotubes is essentially negligible, and molecular motion is therefore dominated by diffusion. Thus this delay between ion current signal and fluorescence signal reflects the time taken for the dye to diffuse from the end of the SWCNT to focal point of the microscope (distance x, Figure S4). To see why the field is negligible, consider the ratio of the voltage drop across the reservoir to that across the CNT which is

$\frac{l_R A_C}{l_C A_R}$ where l_R and l_C are the lengths and A_R and A_C the cross sectional areas of the reservoir and CNT respectively (for a more detailed calculation that takes account of electroosmosis see the SI of Pang et $al.$[8] -electroosmotic flow reduces the estimated field in the CNT still further). Referring to FigureS4, this ratio is ~10^{-8} so the field in the reservoir is ~mV/m and the corresponding drift velocity tens of pm/s (we used a diffusion constant of 4×10^{-10} m^2/s to calculate mobility). This same value of diffusion constant predicts a delay time of ~0.25s for the data in Figure 3D (x=10 μm) and 0.1s for the data in Figure 4D (x=6 μm), values that are consistent with the peak in the measured distributions of delay times.

Do these fluorescence bursts correspond to single molecule signals? This question is best answered with fluorescence correlation spectroscopy measurements of the molecular diffusion constants, but it is impossible to gather enough data from the SWCNT devices to do this. Instead, we measured the fluorescence signals from 40 μl drops of dye solutions on the same coverslips used to make the devices. Single-exponential decay was observed (Figures 5C and F) yielding diffusion constants for the two dyes in excellent agreement with published values (Alexa 546[20], D= 3.5×10^{-10}m^2/s, R6G[21], D= 4.0×10^{-10}m^2/s). The corresponding amplitude and pulse-width distributions are shown in Figures 5A (Alexa 546) and 5D (R6G). These distributions are almost identical to the distributions measured for fluorescence signals obtained from the SWCNT devices (Figures 5B (Alexa 546) and 5E (R6G)). Thus we conclude that each of the fluorescence bursts corresponds to a signal from a single dye molecule.

Since each burst of fluorescence is generally associated with one current spike, we can conclude that each ion current spike signals the passage of a single dye molecule through the SWCNT.

Interestingly, both signs of charge on the dye (R6G, +, Alexa 546, −) produce increases in ion current on translocation. Modeling of DNA translocation in a SWCNT showed that selective ion filtering by the DNA molecule in the SWCNT causes the charge imbalance that increases electroosmotic ion current.[16] Specifically, the negative charge on DNA repels anions, increasing the excess positive charge in the tube. Similarly a positive ion in the tube would increase the excess of anions, so increasing the negative current. Thus, if the charged molecule dominates the process of charge selection in the tube, both positive and negative molecules will result in a current increase. Specifically, the positively charged R6G will block cations, increasing the negative current, while the negatively charged Alexa 546 will block anions, increasing the positive current. There is, however an asymmetry between the two cases because the tubes appear to carry an intrinsic negative charge (likely owing to carboxylate residues).[8] For this reason, tubes containing electrolyte only behave like p-type FETs with a cation excess in the tube.[8] A positive molecule in the tube (R6G) must overcome this background charge, so one might expect the current pulses to be somewhat

smaller in amplitude than is the case for a negative ion. There is some hint of this in the data (Table 1) though tube-to-tube variations probably preclude a firm conclusion on this point.

Conclusion

Carbon nanotubes can be used to build devices that give large signals for the translocation of a single small charged molecules because of the amplification of the ion current signature produced by electroosmosis coupled to charge-filtering by the molecule itself. The data presented here show that each current spike corresponds to the translocation of a single molecule. Furthermore, the fact that both positively and negatively charged molecules lead to increases of current (as opposed to current blockades) implies that the molecule itself is acting as the "charge filter" that generates the spike as the result of an unbalanced electroosmotic flow. We have built gated devices[8] and these might be used to control molecular flow, but cover glasses are not a robust enough platform for these more complex devices.

Methods

Detection of single molecule fluorescence requires the use of a high numerical aperture objective, and these objectives are typically matched to standard 0.16 mm thick cover glasses. Optical losses were too high to observe single molecule fluorescence when we built devices on quartz substrates[22] and the cover glasses are too fragile to serve as substrates for CVD growth of SWCNTs. To solve this problem, we grew carbon nanotubes on a silicon wafer and transferred them onto a standard 0.16 mm thick cover glass (VWR Inc.).[23] SWCNTs were grown by CVD with a ferritin based iron nanoparticles as a catalyst as described elsewhere.[24] They were covered with an e-beam evaporated 20 nm thick SiO_2 layer and then spin-coated with 800nm of Poly (methyl methacrylate, PMMA). After soft baking (170C, 15 min) the PMMA (with the 20 nm SiO_2 layer and embedded SWCNTs) was peeled from the silicon substrate by soaking in 1M KOH aqueous solution at 80°C and transferred onto the cover glass where it was baked at 300°C in an argon flow for 45min. [23] The PMMA layer was decomposed and removed so that the position of the SWCNTs could be recorded relative to alignment markers on the cover glass (Figures 1B and S1). AFM and TEM images showed that the tubes were predominantly single walled with a diameter of 2 ± 0.8 nm.[7] The devices were then spin-coated again with 800 nm of PMMA, after which E-beam lithography was used to cut fluid reservoirs along the path of the nanotubes using the alignment markers and the previously-recorded positions of the SWCNTs. [7] A buffered oxide etch (BOE) was used to remove the 20 nm SiO_2 layer in the reservoirs after which an oxygen plasma was used to open the exposed SWCNT.[7,9] The overall layout of the device is shown in Figure 1A, with a typical ion current-voltage curves shown in Figure 2A. The barrier between reservoirs was 20–30 µm wide, big enough that plasma etching does not cause leakage. However, we checked for leakage through the barriers using control devices lacking a CNT connecting the reservoirs. Only reservoirs connected by a SWCNT showed ionic conductance. Furthermore, the dependence of conductance on salt concentration showed the unusual power-law dependence (Figure 2B) that is characteristic of electroosmotic flow through a SWCNT.[7, 9]

1 mM solutions of Rhodamine 6G (R6G, Aldrich) and Alexa546 C_5 Maleimide (Alexa546, Invitrogen) were prepared with Nanopure water and subsequently diluted to ~ 100 nM in 1M KCl with 1mM phosphate buffer (pH=7) and passed through a 0.02 µm filter (Agilent Technologies Nylon Econofilter). The structure of these dyes is shown in Figure S5, and salt dependence of their fluorescence is given in Figures S6 and 7.

The device was mounted on the sample stage of a Nikon Eclipse TE2000-U inverted microscope with an oil-immersion lens (NA=1.3, 100X, WD= 0.17mm) focused into the reservoir a few microns from the end of the SWCNT (Figure S4). Samples were excited using 0.14 to 0.15 mW of the 514.5 nm line of an argon laser (Melles Griot 43 series). The distance from the end of the reservoir to the collection point varied between about 5 and 10 μm depending on the amount of stray fluorescence and scattering from the walls of the device and its PDMS cover. Sample fluorescence was collected by the same objective (Figure 1A) and passed through a 540–620nm band pass filter for detection by a photon counting module (EG&G Canada SPCM-AQR-14). Optical signals and current signals were acquired simultaneously *via* a Labview data acquisition system running custom software.

Ion current signals were acquired with an Axopatch 200B (Axon Instruments) interfaced to a Labview data acquisition card.

Supplementary Material

Refer to Web version on PubMed Central for supplementary material.

Acknowledgments

References

1. Hinds BJ, Chopra N, Rantell T, Andrews R, Gavalas V, Bachas LG. Aligned Multiwalled Carbon Nanotube Membranes. Science. 2004; 303:62–65. [PubMed: 14645855]

2. Majumder M, Zhan X, Andrews R, Hinds BJ. Voltage Gated Carbon Nanotube Membranes. Langmuir. 2007; 23:8624–8631. [PubMed: 17616216]

3. Lee CY, Choi W, Han JH, Strano MS. Coherence Resonance in a Single-Walled Carbon Nanotube Ion Channel. Science. 2010; 329:1320–1324. [PubMed: 20829480]

4. Fornasiero F, Park HG, Holt JK, Stadermann M, Grigoropoulos CP, Noy A, Bakajin O. Ion Exclusion by Sub-2-nm Nanotube Pores. Proc Natl Acad Sci (USA). 2008; 105:17250–17255. [PubMed: 18539773]

5. Holt JK, Park HG, Wang Y, Stadermann M, Artyukhin AB, Grigoropoulos CP, Noy A, Bakajin O. Fast Mass Transport Through Sub–2-Nanometer Carbon Nanotubes. Science. 2006; 312:1034– 1037. [PubMed: 16709781]

6. He J, Liu H, Pang P, Cao D, Lindsay S. Translocation Events in a Single-Walled Carbon Nanotube. J Phys: Condens Matter. 2010; 22:454112–454118. [PubMed: 21179393]

7. Liu H, He J, Tang J, Liu H, Pang P, Cao D, Krstic PS, Joseph S, Lindsay S, Nuckolls C. Translocation of Single-Stranded DNA through Single-Walled Carbon Nanotubes. Science. 2010; 327:64–67. [PubMed: 20044570]

8. Pang P, He J, Park JH, Krstic PS, Lindsay S. Origin of Giant Ionic Currents in Carbon Nanotube Channels. ACS Nano. 2011; 5:7277–7283. [PubMed: 21888368]

9. Cao D, Pang P, He J, Luo T, Park JH, Krstic P, Nuckolls C, Tang J, Lindsay S. Electronic Sensitivity of Carbon Nanotubes to Internal Water Wetting. ACS Nano. 2011; 5:3113–3119. [PubMed: 21452854]

10. Cao D, Pang P, Liu H, He J, Lindsay SM. Electronic Sensitivity of a Single-Walled Carbon Nanotube to Internal Electrolyte Composition. Nanotechnology. 2012; 23:085203–085209. [PubMed: 22293518]

11. Ito T, Sun L, Crooks RM. Observation of DNA Transport through a Single Carbon Nanotube Channel Using Fluorescence Microscopy. Chemical Communications. 2003:1482–1483. [PubMed: 12868714]

12. Li Y, Chen S, Kaneko T, Hatakeyama R. Electrically Moving Single-Stranded DNA into and out of Double-Walled Carbon Nanotubes. Chemical Communications. 2011; 47:2309–2311. [PubMed: 21152585]

13. Majumder M, Chopra N, Hinds BJ. Mass Transport through Carbon Nanotube Membranes in Three Different Regimes: Ionic Diffusion and Gas and Liquid Flow. ACS Nano. 2011; 5:3867–3877. [PubMed: 21500837]

14. Sun X, Su X, Wu J, Hinds BJ. Electrophoretic Transport of Biomolecules through Carbon Nanotube Membranes. Langmuir. 2011; 27:3150–3156.

15. Fan R, Karnik R, Yue M, Li D, Majumdar A, Yang P. DNA Translocation in Inorganic Nanotubes. Nano Lett. 2005; 5:1633–1637. [PubMed: 16159197]

16. Park JH, He J, Gyarfas B, Lindsay S, Krsti PS. DNA Translocating Through a Carbon Nanotube Can Increase Ionic Current. Nanotechnology. 2012; 23:455107–455113. [PubMed: 23090315]

17. Branton D, Deamer D, Marziali A, Bayley H, Benner SA, Butler T, Di Ventra M, Garaj S, Hibbs A, Huang X, et al. Nanopore Sequencing. Nature Biotechnology. 2008; 26:1146–1153.

18. Feil F, Cauda V, Bein T, Brauchle C. Direct Visualization of Dye and Oligonucleotide Diffusion in Silica Filaments with Collinear Mesopores. Nano Lett. 2012; 12:1354–1361. [PubMed: 22195639]

19. Smeets RMM, Keyser UF, Dekker NH, Dekker C. Noise in Solid State Nanopores. Proc Natl Acad Sci (USA). 2008; 105:417–421. [PubMed: 18184817]

20. Petrašek Z, Schwille P. Precise Measurement of Diffusion Coefficients using Scanning Fluorescence Correlation Spectroscopy. Biophysical Journal. 2008; 94:1437–1448. [PubMed: 17933881]

21. Lee J, Lee Y, Kim SW. Measurement of the Diffusion Coefficients of Single Molecules by Using Fluorescence Correlation Spectroscopy with a Software Correlator. Journal of the Korean Physical Society. 2011; 59:31713176.

22. Yuan D, Ding L, Chu H, Feng Y, McNicholas TP, Liu J. Horizontally Aligned Single-Walled Carbon Nanotube on Quartz from a Large Variety of Metal Catalysts. Nano Lett. 2008; 8:2576–2579. [PubMed: 18593204]

23. Jiao L, Fan B, Xian X, Wu Z, Zhang J, Liu Z. Creation of Nanostructures with Poly(methyl methacrylate)-Mediated Nanotransfer Printing. J Am Chem Soc. 2008; 130:12612–12613. [PubMed: 18763767]

24. Li Y, Kim W, Zhang Y, Rolandi M, Wang D, Dai H. Growth of Single-Walled Carbon Nanotubes from Discrete Catalytic Nanoparticles of Various Sizes. J Phys Chem B. 2001; 105:11424–11431.
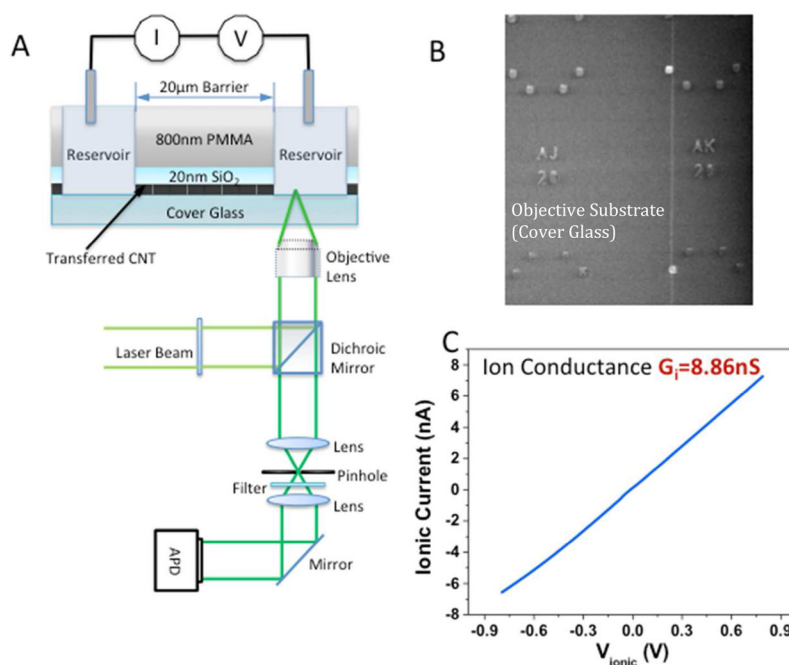
Figure 1.
Apparatus for simultaneous recording of ion current and single-molecule optical signals of translocation through a single carbon nanotube. (A) A laser beam is focused by a high NA objective into an output reservoir coupled to an input reservoir by a single SWCNT that passes through a 20 to 30 micron wide barrier composed of an 800 nm thick PMMA layer on top of a 20 nm thick SiO_2 layer. Charged dye molecules are placed in the input reservoir and driven through the SWCNT by an electric field applied by a pair of Ag/AgCl reference electrodes. The same oil immersion lens collects the fluorescence which is detected by an APD after filtering by a dichroic mirror. (B) SWCNT as transferred onto a 0.16 mm thick cover glass (vertical white line). Index markers on the glass are used to align the fluid reservoirs with the SWCNT. (C) Current-voltage curve for a SWCNT connecting two reservoirs. The conductance is within the range expected for a single 2nm diameter SWCNT with the 1 M KCl used. Current *vs.* salt concentration data (Figure 2) confirm that transport is *via* the SWCNT.
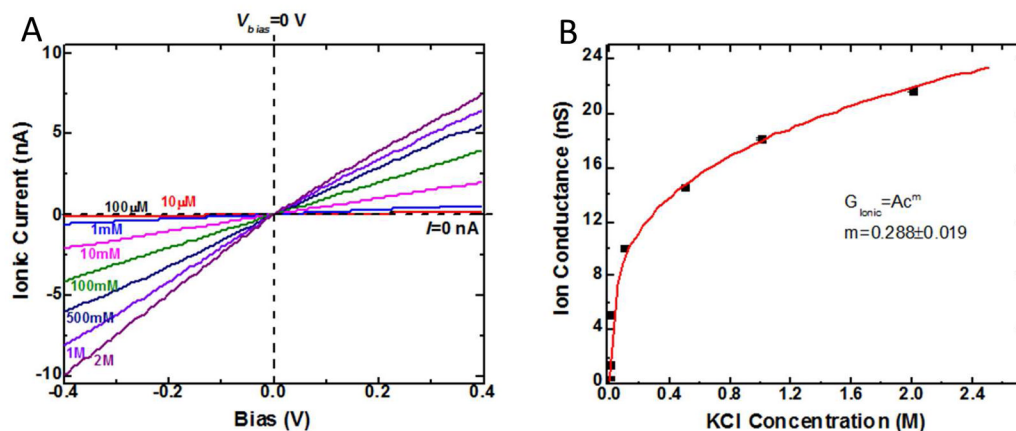
Figure 2.
Current *vs.* voltage for various salt concentrations, *C*, for a SWCNT device on a glass cover slip (A). The slight asymmetry at the highest salt concentration is probably a consequence of the larger surface charge density in these devices compared to devices made with PMMA barriers. Plotted *vs.* concentration (B), the conductance changes according to G~C^m where m~0.3. This is a concentration dependence only observed in ion transport through small-diameter SWCNTs. As we have explained in previous reports[8–10], it is a consequence of significant electroosmotic flow in a very small frictionless channel.
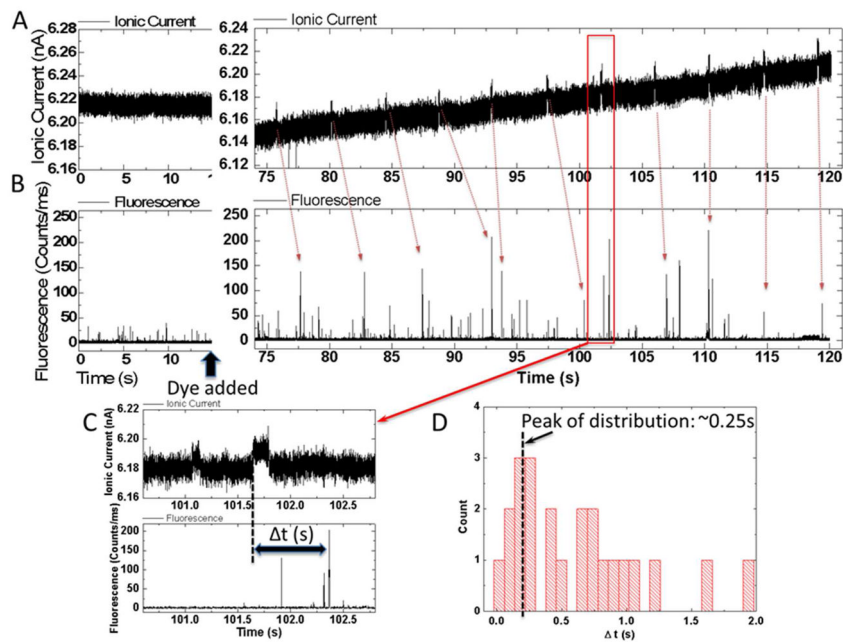
Figure 3.
Simultaneous recordings of current (A) and fluorescence intensity in counts/ms (B) *vs.* time for Alexa 546 dye translocating the device. Panels on the left show data taken before dye is added to the input reservoir. Noise spikes in the ion current are small and of short duration, while the fluorescence noise background rarely peaks above 20 counts/ms. After the addition of dye, current spikes of several tens of pA with durations of a few tenths of a second are observed. They are accompanied by fluorescence spikes of 100–150 counts/ms. These generally follow the ion current signals with a delay (C) of about a quarter of a second (distribution is shown in (D)).
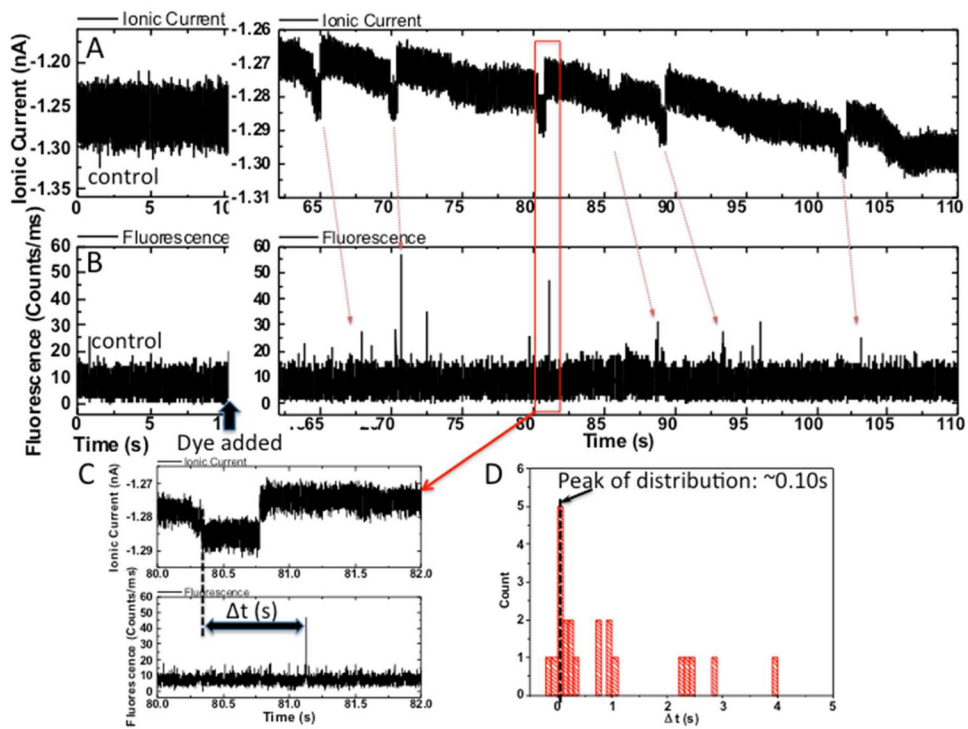
Figure 4.
Data for R6G. Other details are as in Figure 3. Note that the downward going current spikes in (A) correspond to an increase of current.
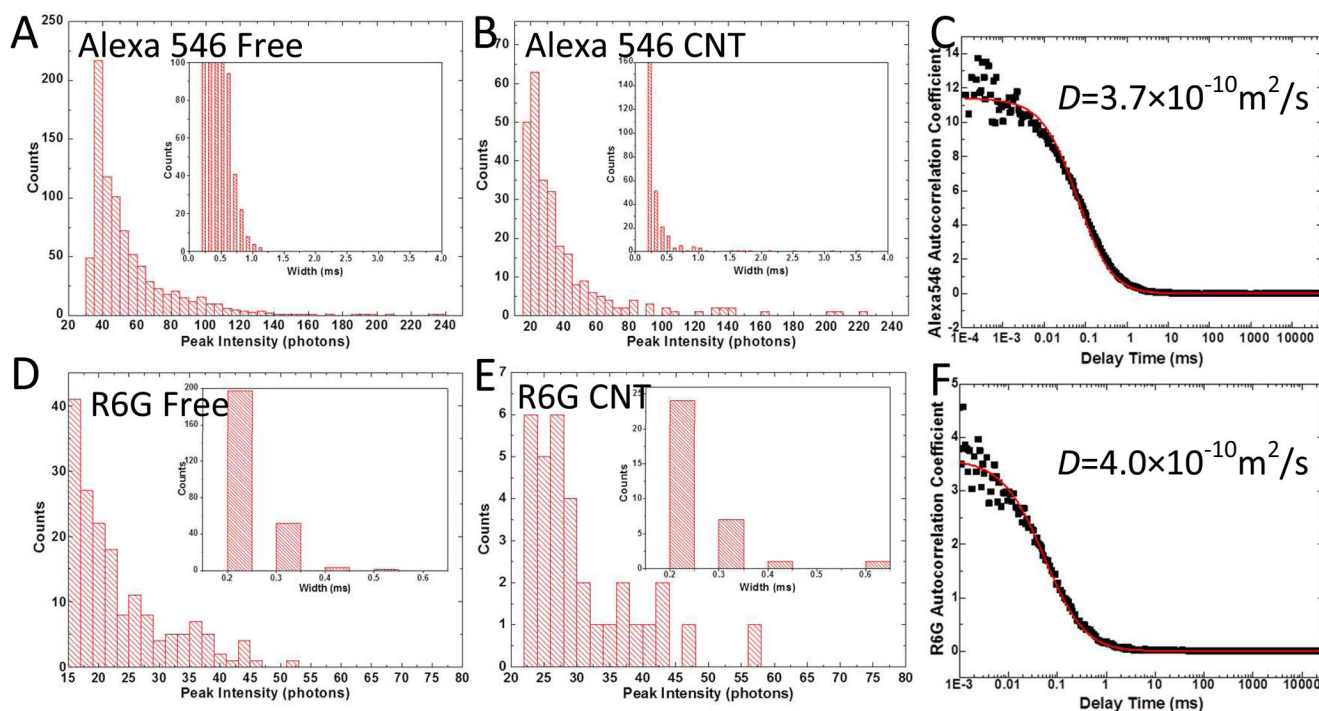
Figure 5.
Comparison of amplitude (signal in counts/ms) and pulse width distributions for solutions (concentration = 90–100 pM for these experiments) of Alexa 546 (A) and R6G (D) with the signals collected in the output devices for the same two dyes (B and E). The histograms are cut off at the baseline noise floor at low peak intensities. The fluorescence autocorrelation functions for the solutions are shown in (C) and (F). Fitted to a single exponential decay time (red lines) they yield the diffusion constants marked, indicating that the fluorescence originates from single molecules.

Table 1

Characteristics of the ion current signals for translocation of two dyes. Scatter plots of amplitude *vs.* decay time are given in Figures S2 and S3.

Dye	Device	Dwell Time (s)	Amplitude (pA)
Alexa 546	1	0.16 ± 0.09	14 ± 4
R6G	2	0.73 ± 0.15	9.1 ± 0.6
R6G	3	0.26 ± 0.06	10.0 ± 0.4